Available online at www.sciencedirect.com
ScienceDirect
Journal of Electroanalytical Chemistry 610 (2007) 37–45
Journal of Electroanalytical Chemistry
www.elsevier.com/locate/jelechem

Evaluation of nanometer thick mercury film electrodes for stripping chronopotentiometry

Luciana S. Rocha [a], José Paulo Pinheiro [b,*], Helena M. Carapuça [a]

[a] Department of Chemistry/CICECO, University of Aveiro, 3810-193 Aveiro, Portugal
[b] Department of Chemistry and Biochemistry/CBME, University of Algarve, Faculty of Sciences, 8005-139 Faro, Portugal

Received 20 March 2007; received in revised form 7 June 2007; accepted 19 June 2007
Available online 29 June 2007

Abstract

In this work, the performance and applicability of the thin mercury film electrode (TMFE) in the heavy metal speciation, by stripping chronopotentiometry (SCP), were exploited. The TMFE thickness was optimized and a 7.6 nm mercury film was selected. This TMFE was mechanically stable and able to perform 60 SCP consecutive measurements, with no significant variation in the analytical signal of lead(II) (RSD less than 2%). Due to the small electrode thickness the measurements were performed under conditions of complete depletion over a wide oxidation current (I_s) range, i.e., within the interval $[75–500]\times 10^{-9}$ A. The limit of detection (3σ) for lead(II) was 2.4×10^{-9} M for a deposition time of 40 s and an oxidation current of 75×10^{-9} A. The TMFE was successfully applied to the construction of SSCP experimental waves, which were in conformity to those predicted by the theory. The stability constant calculated (K') for the Pb(II)-carboxylated latex nanospheres system using a TMFE, agreed with the one obtained using the HMDE, for identical experimental conditions.

Keywords: Thin mercury film electrode; Stripping chronopotentiometry; Scanned stripping chronopotentiometry; Trace metal speciation; Latex nanospheres

1. Introduction

It has long been recognized that the speciation of trace metals play a key role in determining their bioavailability and toxicity in environmental compartments [1,2]. Nevertheless, there remains a lack of experimental methodologies that allow a prompt and reliable quantification and prediction of metal ion complexation, under environmentally relevant conditions (low levels of metallic species) [3,4]. Thus, there is an increasing interest in, and demand for, the development of methods capable to perform trace metal speciation in environmental and biological matrices [5].

Electrochemical methods, in particular stripping techniques are of particular utility for studies on metal ion speciation [3]. This is especially due to their excellent detection limits and their sensitivity to the presence of different metal species [1,2,6]. Anodic stripping voltammetry (ASV) coupled to the hanging mercury drop electrode, HMDE, or to micrometer thick mercury films, MFE, has been widely used in trace metal speciation studies providing information on the stability, lability and mobility of all species present [6]. However, many problems have been reported in its application to environmental matrices containing high levels of organic matter, mainly due to the adsorption of different species onto the electrode surface. This, hinder data interpretation, since the analytical signal is not a reliable representation of the speciation in the sample solution [7,8].

Stripping chronopotentiometry (SCP) is a valuable alternative to ASV [9]. In this technique, the reoxidation of the accumulated metal is carried out by application of a constant oxidising current until full depletion is achieved. The analytical signal is the time needed to reoxidise the

* Corresponding author. Tel.: +351 289 800905; fax: +351 289 819403.
E-mail address: jpinhei@ualg.pt (J.P. Pinheiro).

0022-0728/$ - see front matter © 2007 Elsevier B.V. All rights reserved.
doi:10.1016/j.jelechem.2007.06.018

amalgamated metal, i.e., the transition time, τ. The main advantage of SCP over ASV is the capacitive charge discrimination, by measuring the area under the dt/dE vs E peak that allows the elimination of adsorption complications [10]. The use of the peak area in SCP, under conditions of full depletion, provides the correct measure of the analytical signals in those cases where peak broadening arises from heterogeneity of metal complexes and/or adsorption of organic matter on the electrode surface during the stripping step [10,11]. For improving sensitivity in SCP low stripping currents must be used. In this situation, a significant contribution of traces of dissolved oxygen to the metal oxidation may occur [9].

Scanned stripping chronopotentiometry (SSCP) derived from SCP to provide a fully theoretical supported way to interpret metal complexation parameters. Now, the potentiometric curves are plots of the transition time, τ, as a function of the applied deposition potential, E_d [3]. SSCP curves are inherently rich in information, providing data on the stability distribution spectrum and, if applicable, on the corresponding fraction of the rate constant distributions [3,12–14].

SCP and SSCP are typically performed on mercury electrodes, being the hanging mercury drop electrode (HMDE) and the mercury microelectrode over a supporting iridium micro-disk, currently used in speciation studies. There are some disadvantages associated with these electrodes, namely the ill-defined hydrodynamic regime during the deposition step for the HMDE and the lower sensitivity of the mercury microelectrode. Serrano et al. [15] exploited the application of a micrometer tick mercury film electrode (MFE), in SCP experiments. For that MFE the regime for total depletion could be applied in a wide range of oxidation currents and the hydrodynamic conditions during the deposition step were well defined though there were important disadvantages, namely lack of reproducibility and a complex preparation procedure [15,16].

Recently, thin mercury film electrodes (TMFE) of nanometer thickness were prepared and tested for application in ASV. Stable TMFE could be easily plated (ex situ or in situ mode), by a single electrodeposition step of high overpotential, in acidic solutions containing thiocyanate anion. In these conditions homogeneous and stable mercury deposits of high reproducibility could be prepared [17].

The main objective of the present article is to exploit the features of the thin mercury film electrode (nanometer thickness) in studies of metal ion speciation by SCP/SSCP and elucidate the complementary information that it can provide. The thickness of the mercury electrode was optimized, in order to produce a mechanically stable TMFE, capable to perform c.a. 50–70 consecutive SCP measurements. Afterwards, the SCP complete depletion regime was established and the experimental conditions were optimized (oxidising current, deposition time and metal concentration). Additionally the TMFE was also used in SSCP to evaluate both the repeatability and reproducibility of SSCP experimental waves. Also, its applicability to the determination of metal speciation parameters was accessed, for the metal-complex system Pb(II)-carboxilated latex nanospheres.

2. Theory

2.1. Depletive stripping chronopotentiometry (SCP) at the rotating TMFE

In the depletive regime the number of moles deposited equals:

$$N_{\text{deposited}} = \frac{I_d^* t_d}{nF} \tag{1}$$

and the number of moles reoxidised is given by

$$N_{\text{oxidised}} = \frac{I_s \tau^*}{nF} \tag{2}$$

where I_s is the stripping current, and τ is the limiting value for the transition time obtained for deposition potentials much larger than the standard potential, $E_d \ll E^0$. In the depletion mode, the number of deposited moles equals the number of moles reoxidised and the limiting transition time is given by

$$\tau^* = I_d^* t_d / I_s \tag{3}$$

representing the charge balance for complete depletion [13].

2.2. Scanned stripping chronopotentiometry at the TMFE

The SSCP curves are plotted from a series of measurements made over a range of deposition potentials, E_d. The potential is held at E_d during the deposition time, t_d, after which the oxidising current is applied until all the metal is reoxidised.

Metal-only case SSCP [3,15,18]

For a given potential, the deposition current, I_d, at a rotating TMFE is given by

$$I_d = (nFAD_M(c_M^* - c_M^0))/\delta_M \tag{4}$$

where c_M^* is the metal concentration in the bulk solution, c_M^0 is the metal surface concentration and δ_M is the Nernst diffusion layer thickness. For the rotating disk electrode (RDE) the last parameter is expressed by

$$\delta_M = 1.61 D_M^{1/3} \omega^{-1/2} \upsilon^{1/6} \tag{5}$$

being ω and the angular speed rotation for the RDE ($\omega = 2\pi v_{rot}$, where v_{rot} is the speed of rotation) and υ the viscosity coefficient of the test solution. The other symbols in Eq. (5) have their usual meaning. The limiting value of the deposition current, I_d^*, obtained at large negative potentials at which the concentration of metal ion at the electrode surface is essentially equals to zero ($c_M^0 \to 0$), is given by

$$I_d^* = (nFAD_M c_M^*)/\delta_M \tag{6}$$

Using Eqs. (3) and (6) it is possible to determine the equivalent surface area of the TMFE, A.

The equation that fully describes the relation between τ and E_d (SSCP curve) for the rotating TMFE in the full depletion regime, is equal to that of the conventional HMDE, is given by

$$\tau = (I_d^*\tau_d/I_s)[1 - \exp(-t_d/\tau_d)] \quad (7)$$

in which the characteristic time constant of the deposition process, τ_d, is defined by

$$\tau_d = V_{Hg,dep}/(AD_M\theta\delta_M) \quad (8)$$

where θ the free metal surface concentration ratio ($\theta = c^0_M/c^0_{M^0}$). For a reversible electron transfer reaction, $M + ne^- \leftrightarrow M^0$, and a given deposition potential, E_d

$$\theta = \exp(nF(E_d - E^0)/RT) \quad (9)$$

Assuming a thin-film condition, the volume of the electrode, $V_{Hg,dep}$, can be estimated from the amount of charge of mercury using the Faraday law and assuming the Hg atomic radius as 1.44×10^{-10} m [17]

$$V_{Hg,dep} = \frac{(4/3)\pi r^3_{Hg} N_a Q_{Hg}}{2F} \quad (10)$$

SSCP in labile systems with $D_{ML} < D_M$ [3,12]

Considering the formation of a labile 1:1 metal complex, ML, between the electroactive metal ion M and the ligand L

$$\begin{array}{l} M + L \overset{K_a}{\rightleftarrows} ML \\ \downarrow\uparrow_{ne^-} \\ M^0 \end{array} \quad (11)$$

the stability constant, K, is defined by $K = c_{ML}/(c_M\ c_L)$. For labile complexes, the rates of dissociation/association are sufficiently high relative to the experimental timescale, in order to maintain full equilibrium between complexed and free metal. Under conditions of sufficiently excess of ligand (as typically used in stripping experiments) we can define $K' = Kc^*_{L,t}$ (where $c^*_{L,t}$ is the total concentration of L in the bulk solution). Thus, we can write

$$\theta = (c^0_{M,t}/c^0_{M^0})/(1 + K') \quad (12)$$

where $c_{M,t}$ is the total metal concentration.

If the diffusion coefficient of the metal-complex species (D_{ML}) is lower than that of the free metal ion (D_M), i.e. $D_{ML} < D_M$, the deposition current and τ_d, are modified since D_M is replaced by

$$\overline{D} = \frac{D_M c^*_M + D_{ML} c^*_{ML}}{c^*_{M,t}} \quad (13)$$

and the corresponding diffusion layer thickness, $\bar{\delta}$, is modified accordingly for the given hydrodynamic conditions

$$\bar{\delta} = 1.61\overline{D}^{1/3}\omega^{-1/2}\upsilon^{1/6} \quad (14)$$

The expression for τ_d (former Eq. (8)) thus becomes:

$$\tau_d = V_{Hg,dep}/(A\overline{D}(1 + K')\theta\bar{\delta}) \quad (15)$$

The equation for the SSCP wave for a labile complex ML, τ, is given from Eq. (7), though substituting I^*_d by $I^*_{d,M+L}$, that is expressed by $I^*_{d,M+L} = \tau^*_{M+L}I_s/t_d$ (τ^*_{M+L} is the limiting SCP transition time obtained from of the SSCP curve in the presence of a ligand). The coefficient in Eq. (7), $I^*_d\tau_d/I_s$, is a factor that does not affect the position of the wave on the E_d-axis [3]. Therefore, an explicit expression for the shift of the half-wave potential due to the formation of a complex, $\Delta E_{d,1/2}$ (equivalent to the DeFord–Hume expression) can be obtained considering only the exponential term. In the case of a kinetic current, the shape of the SSCP wave remains unchanged and the same approach can be used, yielding [19]

$$\ln(1 + K') = -(nF/RT)\Delta E_{d,1/2} - \ln(\tau*_{M+L}/\tau*_M) \quad (16)$$

3. Experimental

3.1. Reagents

All chemicals were of analytical reagent grade and all solutions were prepared with ultra-pure water (18.3 MΩ cm, Milli-Q systems, Millipore-waters). Sodium chloride, sodium nitrate, potassium chloride, nitric acid 65% (Merck, suprapur), hydrochloric acid 37% (trace select, Fluka) and 1000 ppm Hg and Pb AA-Spectrosol metal ion standards (BDH) were also used. Ferricyanide standard solution (1.929×10^{-3} mol dm^{-3}) in 1.0 mol dm^{-3} KCl was used for chronoamperometry. Nitric acid (1 M) and sodium hydroxide solutions (1 M) were used for pH adjustments. Stock solution of MES 2-(*N*-morpholinoethanesulfonic acid) buffer was prepared from the solid (Merck). Solutions of ammonium acetate (NH_4Ac 1.0 M/0.5 M HCl) pH buffer and ammonium thiocyanate 1.0 M were prepared monthly and used without further purification. Monodisperse carboxylated latex nanospheres were obtained from Ikerlat Polymers (Spain): $a = 40.0$ nm, $c_{L,t} = 5.2 \times 10^{-5}$ mol COOH per gram. These nanospheres were cleaned by the manufacturer, who provided a conductimetric and potentiometric characterization of each sample.

Biohit Proline pipettes equipped with disposable tips were used for appropriate dilutions. All measurements were carried out at room temperature (18–20 °C).

3.2. Apparatus

An Ecochemie Autolab PGSTAT10 potentiostat (controlled by GPES 4.9 software from EcoChemie, The Netherlands) was used in conjunction with a Methrohm 663 VA stand (Methrohm, Switzerland). The three electrode configuration was used comprising a TMFE plated onto a rotating glassy carbon (GC) disk (1.9 mm diameter, Methrom) as the working electrode, a GC rod counter electrode and a double junction $Hg|Hg_2Cl_2|KCl$(3 M) encased in a 0.1 M $NaNO_3$

solution. The electrochemically active surface area of the glassy carbon electrode, (3.098 ± 0.015) mm^2, was measured by chronoamperometry (in 1.929×10^{-3} M ferricyanide/1.0 M KCl solution; two polishing experiments, each with four replicate determinations).

A combined glass electrode (Radiometer Analytical pHC3006-9) connected to a pH meter (Thermo Electron Corporation, Model Orion 3-Start) was used for pH measurements.

3.3. Preparation of the thin mercury film electrode

Prior to coating, the GCE was conditioned following a reported polishing/cleaning procedure [19]. The GCE was polished with an alumina slurry (grain size 0.3 μm, Metrohm) and sonicated in pure water for 60 s, to obtain a renewed electrode surface. Then, an electrochemical pre-treatment was carried out with a multicycle voltammetric scanning (50×) between −0.8 and +0.8 V at 0.1 V s^{-1}, in NH_4Ac-HCl solution. These polishing and electrochemical pre-treatments were repeated daily.

The thin mercury film was than ex situ prepared in 0.03–0.12 mM mercury (II) nitrate in thiocyanate media (5 mM, pH 3.4) by electrodeposition at −1.3 V for different deposition times (180, 240 or 360 s) and a rotation rate of 1000 rpm [17,18]. The charge associated to the deposited mercury (Q_{Hg}) was calculated by electronic integration of the linear sweep stripping peak of mercury, for $v = 0.005$ V s^{-1}. The electrolyte solution was ammonium thiocyanate 5 mM (pH 3.4) [17]. The stripping step began at −0.15 V and ended at +0.6 V [20]. All charges quoted were mean values of 3 replicate measurements (RDS < 3%). The thickness and repeatability of the TMFE's were estimated using this mean value of Q_{Hg}.

When not in used the GCE was stored dry in a clean atmosphere [17].

3.4. Optimisation of the thin mercury film electrode

The stability of the pre-plated TMFE of different thicknesses (1.9, 2.4, 3.6 and 7.6 nm) was evaluated following the variation of the square-wave anodic stripping voltammetric (SWASV) signal of Pb(II) in a set of 60 consecutive stripping measurements. In addition, the charge associated to the deposited mercury (Q_{Hg}) was determined for two replicate films prior to the set of ASV experiments. The mean value of Q_{Hg} was compared to the final mercury charge of each film of different thickness, which were used in the set of ASV determinations.

For the SWASV experiments the electrolyte used was a 20 mL $NaNO_3$ 0.01 M solution spiked with 6.00×10^{-8} M Pb(II). The deposition and equilibrium time were 20 and 5 s, respectively, for a deposition potential of −0.8 V and a rotation rate of 1000 rpm. The stripping step was initiated at −0.8 V and ended at −0.15 V. The instrumental parameters in SWASV were: amplitude 0.025 V, frequency 25 Hz and step potential 0.005 V. All solutions were purged with nitrogen for 5 min, prior to the voltammetric experiments and blanked during data acquisition.

3.5. Chronopotentiometric procedures

Stripping chronopotentiometric measurements were carried out in 20 mL 0.01 M $NaNO_3$ solutions spiked with lead(II) as a reference metal ion (concentration of Pb(II) 1.19×10^{-7} M). The following conditions were used: deposition potential, −0.65 V; deposition time ranging from 0 to 300 s; rest time of 10 s for a deposition potential of −0.65 V; oxidising current, 2×10^{-9} A to 500×10^{-9} A, applied in a stripping range from −0.65 V to −0.37 V. All solutions were purged for 60 min in the beginning of every SCP experiment and 60 s (assisted by mechanical stirring of the rotating GCE) after each measurement.

The SSCP waves were constructed from a series of individual SCP measurements, by plotting the peak area as a function of the deposition potential, i.e. $[-0.65, 0.48]$ V. For each point the potential was held at E_d for a deposition period of 40 s, followed by the application of a oxidising current of 75×10^{-9} A (complete depletion), until the potential reached a value that is well passed the transition plateau (−0.37 for Pb at the TMFE).

The stability constant, K, of the Pb(II)-40 nm carboxylated latex nanospheres system was determined by SSCP at the TMFE and HMDE. Two SSCP waves were obtained for Pb(II) (2.42×10^{-7} M in $NaNO_3$ 0.01 M), in the absence and in the presence of an excess of carboxylated latex nanospheres (0.1% w/w). Previous to the addition of the ligand, the solution was set at pH 5.5 using MES 2-(*N*-morpholino-ethanesulfonic acid) buffer.

4. Results and discussion

4.1. Evaluation of the stability and durability of thin mercury film electrodes with different thickness

Electrodeposition of mercury onto glassy carbon in acidic solutions of thiocyanate, provides highly homogeneous and reproducible mercury films of nanometer thickness [17]. In the present work, the performance of this type of TMFE, ex situ prepared in thiocyanate media, was evaluated in order to assess their potential application for SCP/SSCP experiments. A good mechanical stability of the thin mercury films represents a major improvement for the in field application of SCP/SSCP.

The variation of the stripping peak current of lead(II) was evaluated for TMFE's of thickness of 1.9, 2.4, 3.6 and 7.6 nm during 60 consecutive stripping experiments. The amount of deposited mercury (measured as Q_{Hg}) was determined before and after the consecutive stripping measurements, in order to assess the durability of the several TMFE's. Table 1 presents these data.

The decrease in I_{pPb} during the consecutive experiments was smaller for the thicker TMFE. Similarly, the decrease of the Q_{Hg} followed the same trend. These features suggest

Table 1
Variation of I_{pPb} (in percentage values) during 60 consecutive SWASV experiments at TMFE's of different thickness; SW parameters: $E_{dep} = -0.8$ V, $t_{dep} = 20$ s, $a = 0.025$ V, $f = 25$ Hz and $v = 0.125$ V s^{-1}

TMFE thickness (nm)	I_{pPb} variation (%)	Q_{Hg} variation[a] (%)
1.9	−25.2	−17.3
2.4	−17.4	−21.2
3.6	−15.8	−7.2
7.6	−9.0	−1.2

Charge determination (LSV): $E_i = -0.15$ V, $E_f = 0.6$ V and $v = 0.005$ V s^{-1}.
[a] Variation of the charge values, Q_{Hg}, relative to fresh mercury films (cf. Section 3.4).

that the degradation of the thinner mercury films was faster than for the thicker, i.e. the loss of small mercury droplets from the GC surface or their coalescence may have occured.

It must be noted that, the variation in the Q_{Hg} values only assess qualitatively the mechanical stability of the TMFE, since the mercury charge measured before and after the sixty SWASV consecutive experiments, was measured on different mercury films. However, it has been already shown that the mercury film deposits are very reproducible when prepared in thiocyanate media (RSD less than 3%) [17]. In conclusion, by selecting a 7.6 nm thickness mercury film electrode, it was possible to perform daily SSCP experiments with a single mercury deposit. In these conditions, the variation in the I_{pPb} ASV signal for 60 consecutive stripping experiments, was less than 10% and the deviations of the Q_{Hg} values, were smaller than 2%. For that reason, the mechanical stability and durability of the TMFE was considered suitable for the present experimental demands.

4.2. Stripping regime in constant-current SCP using the TMFE

The use of a thin mercury film for SCP shall provide a rapid metal transport during the stripping step and, as a result, the measurements are performed frequently under conditions of complete depletion [18].

In the present study, the influence of the SCP oxidative current (I_s) in the lead(II) signal using a thin mercury film electrode (thickness of 7.6 nm) was evaluated.

Depending on the magnitude of I_s, the prevailing conditions during the stripping step could range from linear diffusion, for high I_s values ($I_s\tau^{1/2}$ constant), to the complete depletion limit for low I_s values ($I_s\tau$ constant) [9,10]. The first step was to establish the oxidation current range, under which the depletion of the metal was complete and where the influence of the dissolved oxygen in solution is minimized.

The SCP signals obtained at the TMFE for the current range $[5–500]\times10^{-9}$ A, were well defined and resolved ($w_{1/2}$ varied between 0.033 and 0.034 V). The results revealed that the depletion of lead(II) during the stripping step from the thin mercury film was essentially complete, in the oxidation current range $[5–500]\times10^{-9}$ A (Fig. 1). Although, for lower stripping currents, the $I_s\tau$ parameter was not held constant due to the interferences caused by the dissolved oxygen in the test solution. The interval of operational I_s values can be precisely defined, evaluating the linearity of the $1/I_s$ vs τ plots (Fig. 2).

Fig. 2b shows that for $1/I_s$ higher than 0.013×10^{-9} A^{-1}, corresponding to a stripping current of 75×10^{-9} A, a deviation to linearity of the τ vs $1/I_s$ plot occured. In fact, a decrease in the SCP signal of lead (τ) occurred and by interpolation of the linear section of the τ versus $1/I_s$ plot ($\tau = 1.825\times10^{-7}\ 1/I_s + 7.602\times10^{-2}$) it was possible to predict this variation. The reduction of the SCP signal tend to be progressively higher for lower I_s values, reaching 81% for a stripping current of 2×10^{-9} A.

The influence of dissolved O_2 in the test solution only became negligible for stripping currents higher than 75×10^{-9} A, since the chemical oxidation component was insignificant relative to the imposed oxidising current. Accordingly to this results the interval of operational I_s values was set as $[75–500]\times10^{-9}$ A. The stripping current selected for the following studies was 75×10^{-9} A (lowest working I_s value under the present conditions), given that a higher sensitivity was obtained.

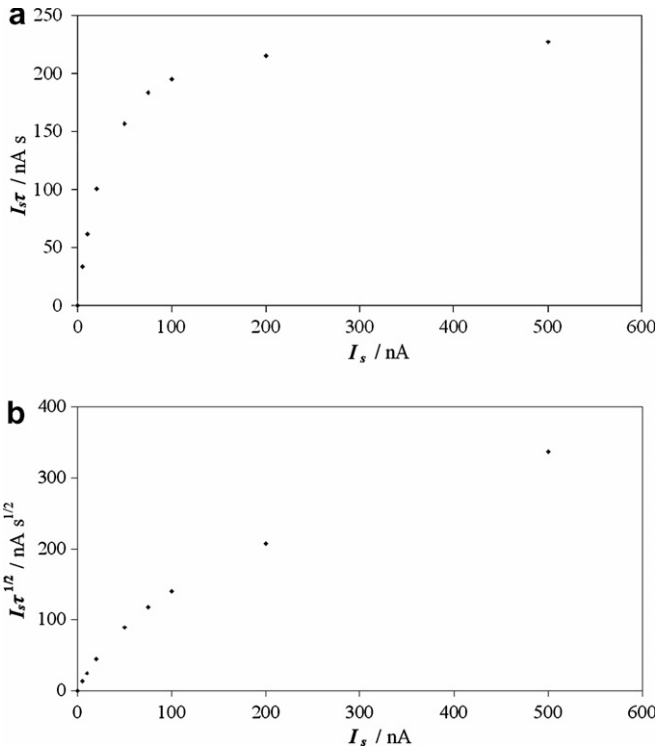

Fig. 1. Evaluation of the SCP stripping regime for a TMFE (thickness 7.6 nm) by plotting: (a) $I_s\tau$ vs I_s (conditions of complete depletion), and (b) $I_s\tau^{1/2}$ vs I_s (conditions of semi-infinite linear diffusion) within the I_s interval of $[0–500]\times10^{-9}$ A. The transition times (τ) were measured in a solution of lead(II) (1.2×10^{-7} M in 0.01 M $NaNO_3$) and for a deposition time of 40 s.

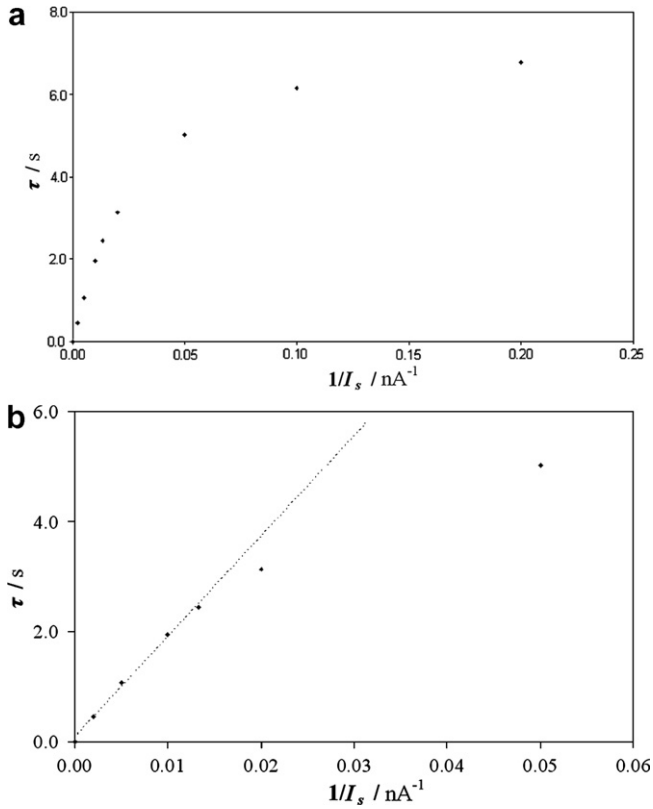

Fig. 2. Effect of the oxidising current (I_s) in the SCP signal of Pb(II) (1.2×10^{-7} M in 0.01 M $NaNO_3$) for a TMFE (thickness 7.6 nm). Deposition time: 40 s. The data are plotted as: τ vs $1/I_s$ for I_s values ranging: (a) $[5–500] \times 10^{-9}$ a and (b) $[20–500] \times 10^{-9}$ A.

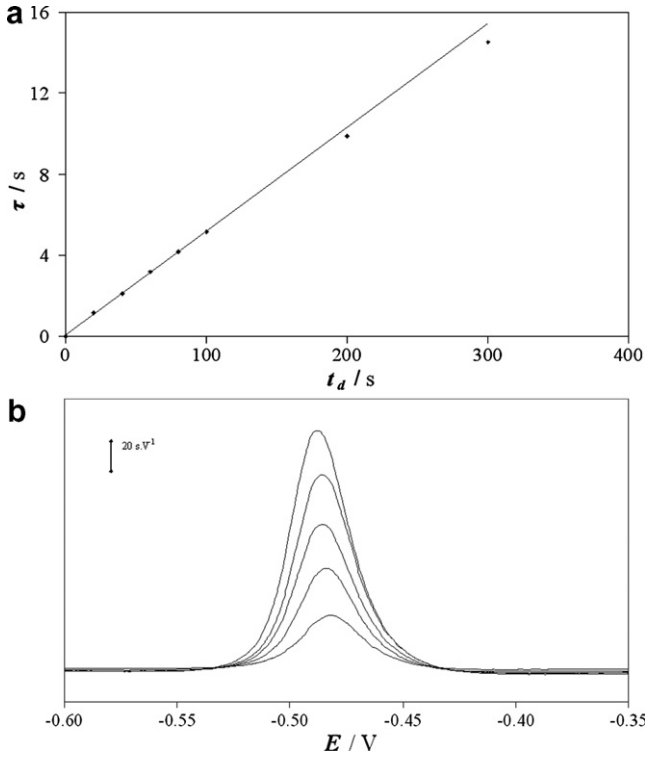

Fig. 3. Effect of the deposition time (t_d) in the SCP signal of lead (τ) at the TMFE (7.6 nm thickness) and for td values of: 20, 40, 60, 80, 100, 200 and 300 s at a deposition potential of −0.65 V. Calibration plot (a) and SCP signals for t_d within the interval of [20–100] s (b). Experiments performed in 0.01 M $NaNO_3$ using a Pb(II) concentration of 1.19×10^{-7} M and a I_s of 75×10^{-9} A.

4.3. Determination of the detection limits for SCP at the 7.6 nm thickness TMFE

Compared to the HMDE, a substantial increase of sensitivity in the stripping measurements was achieved, due to the higher area to volume ratio of the TMFE [18]. However, due to its small volume saturation may occur, for higher metal concentrations or longer deposition times.

To assess these features for the present TMFE (thickness 7.6 nm), the influence of the deposition time (t_d) and the concentration of lead (C_{Pb}) in the SCP signal was studied. Fig. 3 presents the variation of τ with the deposition time, in the interval of [0–300] s for a lead concentration of 1.2×10^{-7} M. All τ values had RSD ranging between 0.1 and 1.6%, evidencing no differences of the repeatability of the SCP signals. The results showed a linear variation of τ with the deposition time within the interval of [0–100] s, with a good definition of the SCP signals, even for lower t_d values (Fig. 3b). Though, a negative deviation to linearity was observed for $t_d \geqslant 200$ s (Fig. 3a), due to a decrease and distortion of the SCP signal, as the thin mercury film began to saturate.

The working concentration range of lead(II) was also evaluated for a deposition time of 40 s. The calibration curve is displayed in Fig. 4a. The linearity was maintained in the concentration interval of $[0–240] \times 10^{-9}$ M. The calibration data were: slope $= 2.28 \times 10^{-2} \pm 1 \times 10^{-4}$ s nM^{-1} and correlation coefficient $= 9.99 \times 10^{-1}$ ($N = 7$; $t_d = 40$ s and a $I_s = 75 \times 10^{-9}$ A). For a lead concentrations above 240×10^{-9} M a negative variation of τ was observed (Fig. 4a). This deviation to the linearity, suggests the beginning of the TMFE saturation. Fig. 4b shows typical signals for the addition of lead in the range $[15–240] \times 10^{-9}$ M.

The saturation occurs at this electrode (TMFE: thickness 7.6 nm; equivalent area 9.38×10^{-6} m^2) for a lead(II) concentration of 1.19×10^{-7} M and within the time deposition interval of [200–300] s or the equivalent combination of this parameters (cf. Eq. (7)). The limit of detection (LOD) for a 40 s deposition time was 2.4×10^{-9} M (3σ) ($N = 7$), however lower values can be achieved by increasing the deposition time (e.g. 1.6×10^{-9} M for 60 s).

The repeatability of the SCP signal of lead(II) at the optimized conditions for a single ex situ formed TMFE, was evaluated for 60 successive measurements (Fig. 5).

A decrease in the transition time of 7.5% occurred during the repeated SCP measurements of lead(II), being the overall RSD less than 2.0%. The stability/durability of the ex situ TMFE used in this set of experiments was also evaluated. The charge associated with this mercury deposit (Q_{Hg}) was compared with a mean value (2 replicates) of

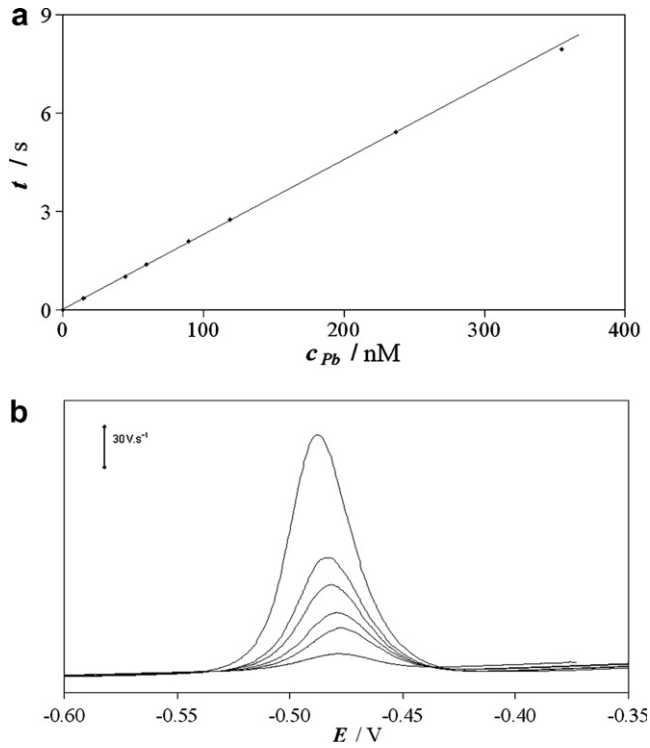

Fig. 4. Variation of the SCP signal (τ) as a function of the concentration of Pb(II) at the TMFE (7.6 nm thickness), for a Pb(II) concentration ($\times 10^{-9}$ M): 15, 45, 60, 89, 120, 240 and 360. Calibration plot (a) and respective SCP signals (b) for a concentration range of $[0–240] \times 10^{-9}$ M. Experiments performed in 0.01 M $NaNO_3$ using t_d of 40 s and a I_s of 75×10^{-9} A.

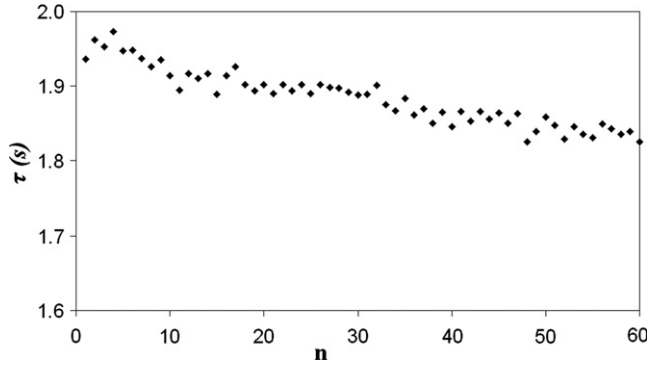

Fig. 5. SCP signal (τ) for repeated measurements ($n = 60$) in a test solution of 1.19×10^{-7} M of lead(II) in 0.01 M $NaNO_3$, at the TMFE (7.6 nm thickness). The other experimental conditions used were: $I_s = 75 \times 10^{-9}$ A and t_d of 40 s.

other pre-plated TMFE's (see Section 3.4). The results pointed out a decrease of 8.5% in the Q_{Hg}. However and according to Section 4.1, this parameter only provides qualitatively information on the conditions of the TMFE. As a result, this nanometer tick MFE is recommended to be used for a maximum of 60 consecutive stripping experiments, revealing no significant alteration in the analytical signal.

4.4. SSCP studies

4.4.1. Experimental verification of the SSCP equation at the TMFE

As far as we know the application of a nanometer tick mercury film as the working electrode for the build up of SSCP curves has never been exploited. The SSCP theoretical curve was calculated using expression (2) (valid for the RDE) for: $E^0 = -0.380$ V, $n = 2$, $D_{Pb} = 9.85 \times 10^{-10}$ m^2 s^{-1} [19], $\delta_{Pb} = 4.93 \times 10^{-5}$ m and $V_{Hg} = 2.35 \times 10^{-15}$ m^3 (deposited Q_{Hg} for 4 replicates measurements was 6.02×10^{-2} C) for the TMFE. The SCP experimental parameters used were: $t_d = 40$ s, $I_s = 7.5 \times 10^{-8}$ and the Pb(II) concentration was of 1.19×10^{-7} mol L^{-1}. The depletive SSCP curve for Pb(II) (calibration) using the TMFE (thickness 7.6 nm) was measured and the experimental results were compared with those calculated from Eq. (4). Fig. 6 shows these results.

The fitting of the SSCP experimental wave using the TMFE was done also, through the analysis of the variation

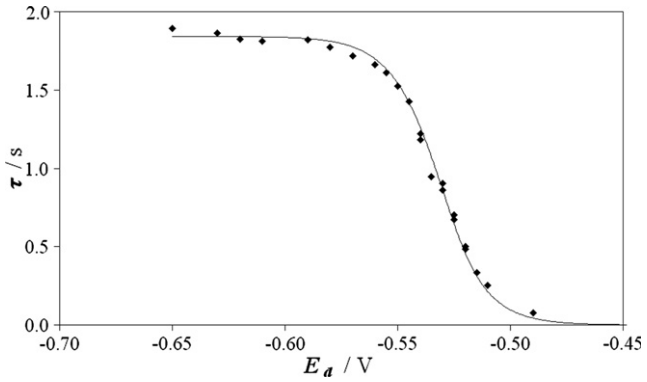

Fig. 6. Experimental (black diamonds) and fitted (full line) SSCP waves for a Pb(II) concentration of 1.19×10^{-7} M at the TMFE (thickness of 7.6 nm). Experimental data was obtained in 0.1 M $NaNO_3$ media at a pH 3.4, using the following SCP experimental parameters: $t_d = 40$ s and $I_s = 7.5 \times 10^{-8}$ A.

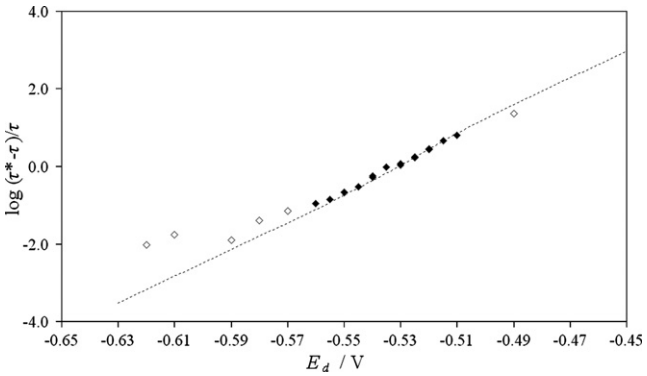

Fig. 7. Log analysis of the experimental SSCP wave (◆ and ◇) for Pb(II) at the TMFE (data presented in Fig. 4). The slope for experimental SSCP curve was determined in the steepest region (◆). Dashed line on the SSCP wave indicates the region of the steepest slope at the foot of the wave.

$\log[(\tau^* - \tau)/\tau]$ vs E_d in the rising portion at the foot of the wave (Fig. 7).

The slope obtained for the $\log[(\tau^* - \tau)/\tau]$ vs E_d plot was of 36.1 ± 0.8 V for the experimental SSCP wave. This value compares very well with the slope obtained for the theoretical SSCP wave, i.e. 36.7 V. In conclusion the experimental SSCP curve was in perfect agreement to that predicted by the theory for the TMFE.

Within the framework of this study one of the most important features to be evaluated was the repeatability of the SSCP curves using the same TMFE. Three experimental SSCP waves were obtained (Fig. 8).

The present results reveal that the SSCP experimental curves were identical within the experimental error, with the limiting transition times, τ^*, of 1.842, 1.865 and 1.851 s and the half-wave deposition potentials, $E_{d,1/2}$, of -0.5300, 0.5295 and -0.5305 V, for wave 1, 2 and 3, respectively. However, the SCCP waves present a slight deviation in the steepest region towards negative potentials. That reflects a decrease in the slope of the $\log[(\tau^* - \tau)/\tau]$ vs E_d plot (36.1 ± 0.8, 35.2 ± 0.5 and 33.5 ± 0.7 for wave 1, 2 and 3, correspondingly). This suggests the beginning of the TMFE degradation which, accordingly to Section 4.3, can be used for a maximum of 60 consecutive experiments. In this study, each SSCP wave was obtained using 28 experimental points and thus, the set of three correspond to 84 measurements. Considering that well defined SSCP waves can be achieved with a set of 15 experiments, four SSCP curves can be obtained per TMFE.

4.4.2. SSCP for metal ion speciation studies: Simple labile system Pb(II)-carboxylated latex nanospheres at the TMFE

The applicability of the TMFE in SSCP experiments for the determination of complexation parameters was evaluated. The Pb(II)-carboxylated latex nanospheres complex was used as a model for the labile metal–ligand system for the determination of the stability constant, K, where $D_{ML} < D_M$. Fig. 9 shows the SSCP waves for lead(II) in the absence and the presence of an excess of carboxylated latex nanospheres (colloidal particle radius of 40 nm), at pH 5.5.

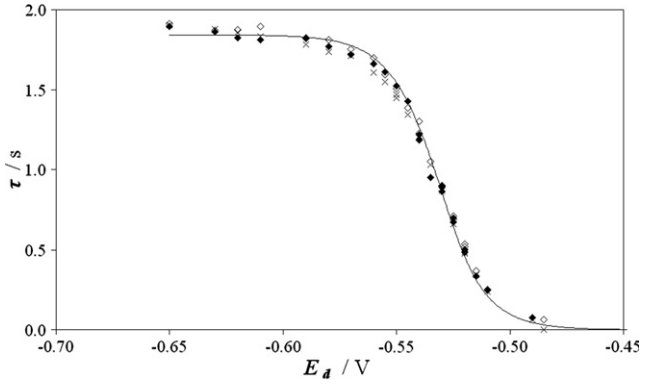

Fig. 8. Fitted (full line) and experimental (◆, ◇ and ×) SSCP waves for a Pb(II) concentration of 1.9×10^{-7} M at the TMFE (thickness of 7.6 nm); the symbols correspond to different SSCP curves performed using the same TMFE: (◆) calibration 1, (◇) calibration 2 and (×) calibration 3. Other conditions as indicated in Fig. 6.

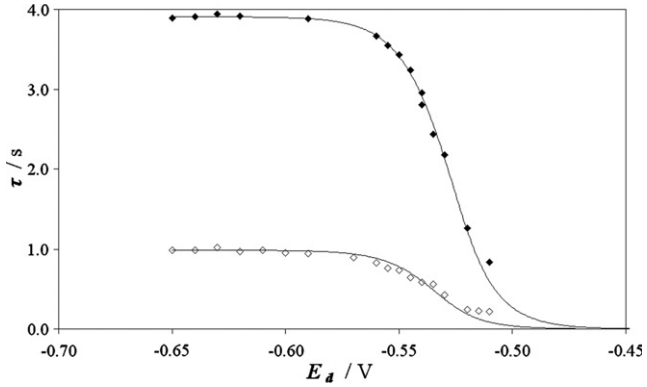

Fig. 9. Experimental (◆ and ◇) and fitted (full line) SSCP waves for Pb(II) and Pb(II)-carboxylated latex nanospheres system at pH 5.5 at the TMFE (thickness of 7.6 nm). Experimental curves were measured for a Pb(II) concentration of 2.4×10^{-7} M in the absence (◆) and presence of the latex nanospheres (◇) at 0.1% (w/w) in 0.01 mol L^{-1} $NaNO_3$. Other parameters: $E^0 = -0.374$ V, $n = 2$, $D_{ML} = 1.26 \times 10^{-10}$ m^2 s^{-1}, $\delta_M = 2.48 \times 10^{-5}$ m and $V_{Hg} = 2.35 \times 10^{-15}$ m^3. Other experimental conditions as indicated in Fig. 6.

The fitted wave for the labile Pb(II)-carboxylated latex nanospheres system, was calculated using Eq. (7). Using Eq. (16) we obtained a K' of 6.7 ± 0.6, which is in reasonable agreement the value of 7.7 ± 0.6 obtained at the HMDE.

Immediately following this work we plan to evaluate the rotating TMFE in SSCP dynamic speciation studies to fully take advantage of the well defined hydrodynamic features of this electrode. We are especially interested in the application in trace metal binding in colloidal dispersions [21–23].

5. Conclusions

The present work reveals that a thin mercury film electrode can be successfully applied in SCP/SSCP studies of heavy metals. The optimized TMFE (film thickness of 7.6 nm) can be use for 1-day term (60 SCP consecutive measurements) with no significant variation in the analytical signal (RSD less than 2%) and no apparent degradation of electrode surface (RSD less than 3% for the Q_{Hg}). Due to the low thickness and volume of this electrode (7.6 nm and 2.4×10^{-14} m^3, correspondingly), the stripping step follows a thin-layer behaviour and, as a result, the depletion effects predominate ($I_s\tau$ regime). Therefore, high stripping currents can be used (I_s values higher than 75×10^{-9} A) preventing dissolved oxygen interference. The SCP signals obtained at the TMFE are narrow and well defined, even when low concentrations of Pb(II) and short deposition times are used, which in turn shorten the analysis times. The limit of detection (3σ) for Pb(II) was 2.4×10^{-9} M using a stripping current of 75×10^{-8} A and a deposition time of 40 s.

The calculated SSCP curves are in excellent agreement with experimental data for Pb(II) at the TMFE. A single TMFE can be used to obtain four identical and well defined SSCP curves, each one with 15 experimental points (15 individual SCP measurements). Furthermore, the stability constant (K') of the Pb(II)-carboxylated latex nanospheres system, calculated from the shift in the SSCP half-wave potential ($\Delta E_{1/2}$) at the TMFE, is in reasonable agreement to the one obtained with the HMDE, in identical experimental conditions.

The high sensitivity and resolution obtained at the TMFE and also the low deposition times which in turn are used, made this electrode an excellent complement to the conventional mercury electrodes.

Acknowledgements

Thanks are due to University of Aveiro and Fundação para a Ciência e a Tecnologia (FCT) project POCI/AMB/55939/2004. Luciana Rocha acknowledges FCT, for a PhD grant.

References

[1] A. Tessier, D.R. Turner, Metal Speciation and Bioavailability in Aquatic Systems, vol. 3, John Wiley & Sons, 1995 (chapter 5).
[2] T.M. Florence, Talanta 29 (1982) 345.
[3] H.P. van Leeuwen, R.M. Town, J. Electroanal. Chem. 536 (2002) 129.
[4] R.M. Town, H.P. van Leeuwen, Electroanalysis 16 (2004) 458.
[5] M.-L. Tercier-Waeber, J. Buffle, F. Confalonieri, G. Riccardi, A. Sina, F. Graziottin, G.C. Fiaccabrino, M. Koudelka-Hep, Meas. Sci. Technol. 10 (1999) 1202.
[6] A.M. Ure, C.M. Davidson, Chemical Speciation in the Environment, Blackie Academic & Professional, Chapman & Hall, 1995 (chapter 2.7).
[7] M.L. Tercier, J. Buffle, Anal. Chem. 68 (1996) 3670.
[8] G.E. Batley, T.M. Florence, Electroanal. Chem. Interf. Electrochem. 55 (1974) 23.
[9] R.M. Town, H.P. van Leeuwen, J. Electroanal. Chem. 509 (2001) 58.
[10] H.P. van Leeuwen, R.M. Town, J. Electroanal. Chem. 523 (2002) 16.
[11] H.P. van Leeuwen, R.M. Town, J. Electroanal. Chem. 523 (2002) 1.
[12] R.M. Town, H.P. van Leeuwen, J. Electroanal. Chem. 541 (2003) 51.
[13] H.P. van Leeuwen, R.M. Town, Environ. Sci. Technol. 37 (2003) 3945.
[14] J.P. Pinheiro, H.P. Van Leeuwen, J. Electroanal. Chem. 570 (2004) 69.
[15] N. Serrano, J.M. Díaz-Cruz, C. Ariño, M. Esteban, J. Electroanal. Chem. 560 (2003) 105.
[16] D. Jagner, M. Josefson, S. Westerlund, Anal. Chem. 53 (1981) 1406.
[17] S.C.C. Monterroso, H.M. Carapuça, J.E.J. Simão, A.C. Duarte, Anal. Chim. Acta 503 (2004) 203.
[18] A.J. Bard, L.R. Faulkner, Electrochemical Methods – Fundamental and Applications, second ed., Wiley, 2001 (chapter 11–12).
[19] S.C.C. Monterroso, H.M. Carapuça, A.C. Duarte, Electroanalysis 15 (2003) 1878.
[20] L.S. Rocha, H.M. Carapuça, J.P. Pinheiro, Langmuir 22 (2006) 8241.
[21] J.P. Pinheiro, M. Minor, H.P. van Leeuwen, Langmuir 21 (2005) 8635.
[22] J.P. Pinheiro, M. Minor, H.P. van Leeuwen, J. Electroanal. Chem. 587 (2006) 284.
[23] J.P. Pinheiro, R. Domingos, M. Minor, H.P. van Leeuwen, J. Electroanal. Chem. 596 (2006) 57.